

The Proportion of Synapses Formed by the Axons of the Lateral Geniculate Nucleus in Layer 4 of Area 17 of the Cat

NUNO MAÇARICO DA COSTA AND KEVAN A.C. MARTIN

Institute for Neuroinformatics, University of Zürich and ETH Zürich, 8057 Zürich, Switzerland

ABSTRACT

The connection between the dorsal lateral geniculate nucleus (dLGN) and area 17 of the cat is a classical model for studying thalamocortical relations. We investigated the proportion of asymmetric synapses in layer 4 of area 17 of cats formed by axons of the dLGN, because this is an important morphological parameter in understanding the impact of dLGN axons on their target neurons. Although the present consensus is that this proportion is small, the exact percentage remains in doubt. Most previous work estimated that the thalamus contributes less than 10% of excitatory synapses in layer 4, but one estimate was as high as 28%. Two issues contribute to these widely different estimates, one being the tracers used, the other being the use of biased stereological approaches. We have addressed both

of these issues. Thalamic axons were labeled in vivo by injections of biotinylated dextran amine into the A lamina of the dLGN of anesthetized cats. After processing, the brain was cut serially and prepared for light and electron microscopy. The density of asymmetric synapses in the neuropil and the density of synapses formed by labeled dLGN boutons were measured by using an unbiased sampling method called the *physical disector*. Our counts indicate that, in the fixed cat brain, there are $5.9 \times 10^8 \pm 0.9 \times 10^8$ asymmetric synapses per cubic millimeter of layer 4 in area 17, and the dLGN input provides only 6% of all asymmetric synapses in layer 4. The vast majority of synapses of layer 4 probably originate from other neurons in area 17. *J. Comp. Neurol.* 516:264–276, 2009. © 2009 Wiley-Liss, Inc.

Indexing terms: dLGN; electron microscopy; physical disector; visual cortex; synapse density

The major thalamic input to area 17 of the cat originates from the relay neurons of the dorsal lateral geniculate nucleus (dLGN). These neurons relay visual information mainly to visual areas: 17, 18, and 19 (Hollander and Vanegas, 1977; Kawano, 1998; Laemle, 1975; Leventhal, 1979; Maciewicz, 1975). In their insightful model of layer 4 simple cells, Hubel and Wiesel (1962) explained the simple cell structure by the convergence of dLGN afferents on layer 4 neurons. This model remains the textbooks' favorite, and, following Hubel and Wiesel's lead, the thalamocortical projection to primary visual cortex is now widely considered to be the cardinal example of a feedforward "driving" input to cortex (Crick and Koch, 1998; Sherman and Guillery, 1998).

Our own continuing concern, however, is for more precise quantitative estimates of the contribution of the thalamic synapses to visual cortex (Ahmed et al., 1994, 1997; Latawiec et al., 2000), not just because they are needed for us to build much more biophysically and anatomically accurate circuit models (Banitt et al., 2007) but also because understanding how the thalamus interacts with the cortical circuits is of fundamental relevance for all of the neocortex. The visual cortex of cat has been the most intensively studied, and it still offers us the best opportunity to explore the causal links between structure, biophysics, and circuit-level operations

that produce the emergent properties of cortical neurons, such as orientation selectivity.

The detailed anatomical knowledge that has accumulated since Hubel and Wiesel published their model has revealed a paradox: although the receptive fields of simple cells are apparently determined entirely by the dLGN synapses, only a small percentage of all the excitatory synapses in layer 4 actually seem to originate from dLGN neurons. The consensus is that the dLGN provides less than 10% of all the excitatory

Additional Supporting Information may be found in the online version of this article.

Grant sponsor: E.U. Daisy FP6-2005-015803 (to K.A.C.M.); Grant sponsor: Human Frontier Science Program; Grant number RG0123/2000-B (to K.A.C.M.); Grant sponsor: N.M.C. was a fellow from Fundação para a Ciência e Tecnologia in the Gulbenkian PhD Program in Biology and Medicine; Grant number: SFRH/BD/2724/2000.

*Correspondence to: Nuno Maçarico da Costa, Institute for Neuroinformatics, University of Zürich and ETH Zürich, Winterthurerstr.190, 8057 Zürich, Switzerland. E-mail: ndacosta@ini.phys.ethz.ch

Received 11 August 2008; Revised 23 April 2009; Accepted 30 May 2009
DOI 10.1002/cne.22133

Published online June 11, 2009 in Wiley InterScience (www.interscience.wiley.com).

synapses in layer 4 (with one outlier of 28%; LeVay and Gilbert, 1976). However, there were wide differences in experimental methods for identifying thalamic synapses. Some studies used degeneration methods (Garey and Powell, 1971; Hornung and Garey, 1981); some used morphological criteria (Ahmed et al., 1994, 1997) or axonally transported tracers (LeVay, 1986; LeVay and Gilbert, 1976). When sampling methods were reported, the synapses were counted in single sections, which biases the sampling toward larger synapses. To estimate the proportion of synapses originating in the dLGN, the total number of synapses in layer 4 must also be known. Here the counts of Beaulieu and Colonnier (1985) are the most recent and most widely cited, but they have been criticized by Mayhew (1996), because they were based on a flawed model. Thus, for a number of methodological reasons, the proportion of dLGN synapses in the cat may not be entirely reliable.

The situation in the monkey is somewhat clearer. Garey and Powell (1971) applied the same degeneration and sampling methods that they had used in the cat to the monkey and found that 5–10% of the synapses in layer 4C were provided by the dLGN. Later DeFelipe and Jones (1991) discovered that the calcium-binding protein parvalbumin is present in dLGN boutons in primary visual cortex of the monkey, and the convenient presence of this endogenous marker was exploited by Latawiec et al. (2000) to count the dLGN synapses using the unbiased sampling of the physical disector method. Their estimates of 8.7% for layer 4C α and 6.9% for 4C β were surprisingly close to those of Garey and Powell (1971). This raises the interesting question of whether the “old-fashioned” degeneration methods and sampling might actually give reasonably accurate data.

Unfortunately, for the cat, there is no known endogenous marker for the dLGN boutons, but we have revisited the problem of the dLGN fraction using more effective tracers and unbiased sampling methods. Our results show that the dLGN forms 6% of all the asymmetric synapses in layer 4 of area 17, and that Beaulieu and Colonnier's (1985) counts of total synapses are reasonable.

MATERIALS AND METHODS

Surgical procedures

All experiments, animal treatment, and surgical protocols were carried out with authorization and under license granted to K.A.C.M. by the Kantonal Veterinärämteramt of Zurich. The material presented here originates from three male and one female cats. One of the cats was 9 weeks old; the other three were adults with ages ranging from 9 to 19 months. All cats were prepared for surgery after subcutaneous or intramuscular injection of xylazine (Rompun, Bayer; 0.5 mg · kg⁻¹) and ketamine (Narketan 10, Vetoquinol AG, CH; 10 mg · kg⁻¹); additional gas anesthesia with 1–2% halothane (Arovet AG, CH) in oxygen/nitrous oxide (50/50%) was also delivered. After induction of anesthesia, some of the cats received a subcutaneous injection of atropine (Graeub) of 0.05 mg · kg⁻¹, to decrease secretions. All experiments were performed under sterile conditions. The femoral vein was cannulated, and alphaxalone/alphadalone (Saffan; Glaxo) was delivered to maintain anesthesia during the remainder of the experiment. Afterward, the cat was intubated and moved to a stereotaxic apparatus, where it was respired artificially with a mixture of

oxygen/nitrous oxide (30%/70%). The end-tidal CO₂ was maintained at ~4.5%. Lidocaine gel 4% (G. Streudi and Co., AG) was applied to all pressure points. Anesthesia was supplemented with halothane gas during the remainder of the experiment.

Electroencephalogram (EEG), electrocardiogram (ECG), end-tidal CO₂, and rectal temperature were monitored continuously during the entire experiment. A thermister-controlled heating blanket maintained the cat's rectal temperature at 37°C. Topical antibiotics (Voltamicin; Novartis) and atropine 1% (Novartis; to paralyze accommodation) were applied to the eyes before they were covered with gas-permeable contact lenses. One drop of phenylephrine 5% (Blache) was applied to each nictitating membrane in order to retract them.

After surgery, the cats were given an intravenous injection of the muscle relaxant gallamine triethiodide (12 mg induction dose, 5 mg · kg⁻¹ · hour⁻¹ thereafter; Flaxedil; May Balces). This low dose of muscle relaxant was enough to reduce eye movement during the short period of time when the cat was paralyzed. To allow recovery of the animal, delivery of the muscle relaxant was stopped 2–3 hours before the end of the recording and iontophoresis.

After iontophoresis of the tracers into dLGN, the craniotomies were closed by gluing back the original bone flap to the skull with dental cement. A prophylactic dose of antibiotics was administered to the cat both intramuscularly (10 mg · kg⁻¹; Clamoxyl; GlaxoSmithKline) and topically on the skull (Soframycin; Aventis). The skin and head muscles were sutured, and respiration and muscular tonus were monitored to assess the animals recovery. A dose of analgesic (0.01 mg · kg⁻¹ buprenorphinum; Tengesic; Essex Chemie AG.) was administered, and in the 2 days that followed surgery the cat received a subcutaneous injection 10 mg · kg⁻¹ Clamoxyl per day. During the survival period that lasted from 5 to 22 days, the cat was monitored daily to assess whether any signs of pain or infection were visible.

Injections of biotinylated dextran amine in the A lamina of the dLGN

A craniotomy was performed with a trephine centered at Horsley-Clark coordinates anteroposterior (AP) 8–9 and medial-lateral (ML) 5–6. A tungsten electrode insulated with epoxy was positioned in the center of the craniotomy, and, after opening a slit in the dura mater, was lowered into the brain. The position of the dLGN was confirmed electrophysiologically in two ways: first, by the responses of neurons to light flashes to the ipsilateral or contralateral eye, confirming the eye specificity of the different lamina of the dLGN, and, second, by making several penetrations and confirming the map of visual space described by Sanderson (1971). When the A lamina of the dLGN was located, the depth was noted, and the tungsten electrode was replaced by a glass micropipette filled with a solution of biotinylated dextran amine (BDA; MW 10,000; Molecular Probes, Leiden, The Netherlands). The pipette tip diameter varied from 10 μ m to 18 μ m. The A lamina was then found again by recording through the injection pipette. Injections were made iontophoretically, lasting for 15–20 minutes, with current pulses of 3 seconds on/3 seconds off, with an amplitude of 2–4 μ A. The BDA was delivered as a 10% solution in 0.01 M phosphate buffer (PB), pH 7.4; or 0.01 M PB and 0.2 M KCl, or 0.05 M Tris and 0.2 M KCl. Injections were separated by at least 500 μ m, and usually more, so that

the retinotopic progression could be distinguished in the cortex. Most of the injections were aimed at locations near the visual representation of the vertical meridian ($<10^\circ$), which corresponds to the medial edge of the dLGN.

Perfusion

After the survival period, anesthesia was again induced with ketamine/xylazine and the cats were deeply anesthetized with i.v. Saffan (20 mg/kg) until the EEG became flat and the end-tidal CO_2 was lowered to 3.5%. Then, the cat was perfused transcardially with normal 0.9% NaCl solution, followed by a warm solution of 4% paraformaldehyde (w/v), 0.3% glutaraldehyde (v/v), and 15% saturated solution of picric acid (v/v) in 0.1 M PB, pH 7.4. After fixation, the cat was perfused with a solution of 10% and 20% solution of sucrose in 0.1 M PB. The brain was cut stereotaxically, and blocks containing the injected dLGN and area 17 were removed.

Histology

The blocks of brains were allowed to sink in sucrose solutions of 20% and 30% in 0.1 M PB to provide cryoprotection. The blocks were then freeze-thawed twice in liquid nitrogen to enhance the penetration of the avidin-HRP by mechanically disrupting the tissue. The brain blocks were then washed in 0.1 M PB for at least 2 hours to allow them to recover from the shrinkage provoked by the incubation in sucrose solution. Sections were cut from the blocks at 80 μm in the coronal plane and collected in 0.1 M PB. After cutting, the sections were washed several times in buffer to remove any remaining fixative. To reveal BDA, the sections were washed in TBS and then incubated overnight (5°C) with an avidin-biotin complex (Vector ABC Elite kit). The peroxidase activity was identified by using 3-diaminobenzidine tetrahydrochloride (DAB) with nickel intensification. After assessment by light microscopy (LM), regions of tissue were selected for subsequent electron microscopy (EM) analysis. These sections were treated with 1% osmium tetroxide in 0.1 M PB, dehydrated through alcohols (1% uranyl acetate in the 70% alcohol) and propylene oxide, and flat mounted in Durcupan (Fluka) on glass slides. Regions with dense dLGN labels were blocked and cut into ultrathin sections of 60 nm; the sections were then collected on Pioloform-coated single slot copper grids. Sections not selected for EM were air dried, dehydrated through alcohols, and mounted with DPX (Fluka). Sections including the dLGN were stained with neutral red to visualize the different laminae. Shrinkage resulting from the histological procedure was accessed by measuring the cut edge of the osmicated and nonosmicated parts of the section.

Synapse classification

Synapses and associated structures were classified by conventional criteria (Colonnier, 1968; Gray, 1959). Synapses were considered as "asymmetric" (Grays's type 1) when they showed round or spheroidal synaptic vesicles in the presynaptic terminal and a postsynaptic density (PSD), separated by a synaptic cleft. Appositions in which the synaptic cleft was not visible, but where a PSD was present and where synaptic vesicles were in close proximity or in contact with the presynaptic membrane, were considered to be synapses.

Physical disector

The density of asymmetric synapses was estimated by using the physical disector method (Sterio, 1984). Reference and lookup section were separated by one intervening section so that the disector z dimension was 0.120 μm . The density of synapses (N_V) was calculated by using the following formula:

$$N_V = \frac{n}{V_{\text{disector}}}$$

where n is the number of synapses counted, and V_{disector} is the volume of a single disector. The section thickness was measured from approximately half of the reference sections by using Small's fold method (Small, 1968; described by Royet, 1991) to verify that the average section thickness was 60 nm.

Sampling of physical disectors for the density of dLGN synapses

Disectors were sampled by using rare-event systematically optimized random sampling (RESORS; da Costa et al., 2009). The sampling sites are chosen with a systematic random sampling (SRS) scheme (Gundersen and Jensen, 1987; Słomianka and West, 2005), but we photographed and made synaptic counts and measurements only at sampling sites that had a labeled bouton or had a labeled bouton forming a synapse. The density of labeled synapses in the neuropil is then calculated by taking into account the volume of all the sampling sites (i.e., photographed and not photographed). We can also calculate the density of all asymmetric synapses in the neuropil by counting the number of labeled and unlabeled synapses on the photographed sampling sites. The disectors had a size of 5 \times 5 μm and were collected by taking photographs at a magnification of $\times 13,500$ with a digital camera (11 megapixels, Morada; Soft Imaging Systems).

Sampling of physical disectors for the density of asymmetric synapses in the neuropil

Three sampling methods were used. In the first method, serial sections were photographed in the EM with an analog camera at a magnification of $\times 11,500$ and stitched together. The different disector pairs had different sizes but usually formed a strip. In the second method, the location of the disector reference frame within the ultrathin section was taken using a uniform random sampling scheme. Serial sections were photographed in the EM with a digital camera (1.3 megapixels, MegaView III; Soft Imaging Systems) at a magnification of $\times 25,000$ and merged together in Adobe Photoshop CS and CS2. The disector frame had a size of approximately 30 $\mu\text{m} \times 30 \mu\text{m}$.

In the third sampling method, the location of the disector reference frame was chosen with a systematic random sampling scheme. The disectors were collected from every n th grid, the starting grid was chosen randomly from 1 to n , using the Matlab Rand function initialize to a different state every time. On each copper grid, the first section was chosen as the reference of the disector. A sampling grid indicating the location of the several disectors was then randomly positioned on a low-power photograph of the reference section. The disectors had a size of 5 \times 5 μm and were collected by taking photographs at a magnification of $\times 13,500$ with a digital cam-

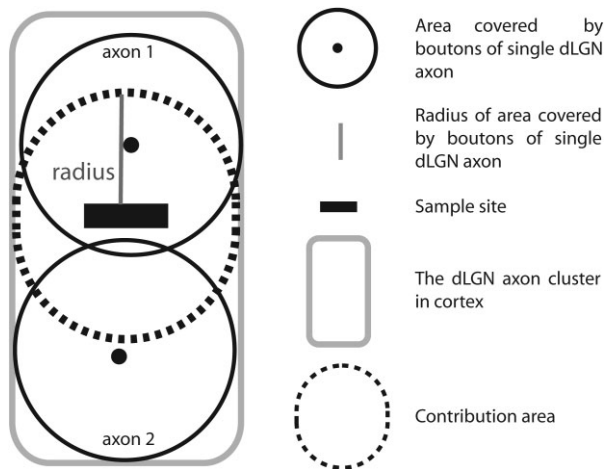


Figure 1. Description of the steps taken to calculate the contribution area (dotted line) of dLGN axons to the region of the cortex (rectangle) sampled with physical disectors. This figure shows a surface view of the cortex. Only axons inside the cluster of dLGN axons representing one eye (gray line) and located at a distance inferior to the radius of its coverage can contribute (axon 1) with boutons to the gray region.

era (11 megapixels, Morada; Soft Imaging Systems). Adobe Photoshop CS4 was used for histogram equalization and contrast enhancement in digital photomicrographs. Adobe Illustrator CS4 was used to prepare the figures.

Estimation of number of dLGN neurons contributing boutons to the volume sampled by the physical disectors

Because our injections were punctate, they did not label all cells of the A lamina of the dLGN. We thus assessed the proportion of labeled relay dLGN cells that formed boutons in the region of area 17 where we counted synapses. The method we used was similar to that used by Freund et al. (1985a), Friedlander and Martin (1989), and Peters and Payne (1993) to calculate how many dLGN axons contribute boutons to a single point in cortex and is illustrated in Figure 1. A single dLGN axon has an arbor of a finite diameter that covers a region of the cortex, dLGN axons separated from a sample site by less than the mean radius of their arbor (thus, axon 1 but not axon 2 in Fig. 1) will contribute boutons to that sample site. The surface area of the cortex around a given sample site that has axons contributing boutons to that sample site is called the *contribution area* (region delimited by the dotted line in Fig. 1). This contribution area was calculated separately for X and Y axons. The radius of the dLGN arbor was calculated from the surface area (row 5 and 6 in Table 1). To obtain an estimate of the number of axons, the contribution area was then multiplied by the area density of dLGN axons. The area density was calculated by dividing the total number of relay neurons in A lamina of the dLGN (rows 3 and 4 in Table 1) by half of the surface area of area 17 (row 7 in Table 1).

To estimate how many neurons are labeled by the injection in the dLGN, we reconstructed the core of the injection site and the complete contralateral A lamina of the dLGN in the software Reconstruct (Fiala, 2005). The core was defined as the region of the injection site where almost all neurons are

labeled (over 85%, judged in sections that were counterstained with neutral red, Fig. 2). There were labeled cells outside of the core of the injection site, but these were under 15% of cells.

We then calculated the proportion of the volume of the A lamina occupied by the core of the injection site and thereby the proportion of labeled vs. the total number of relay cells in the A lamina of the dLGN estimated by Madarasz et al. (1978a,b; row 1 in Table 1).

Calculation of the error of the estimation

The error of each of the values entering the calculation of the percentage of dLGN synapses was propagated in quadrature in order to obtain the error of the final estimation. For each value, the error was expressed as the SEM. Whenever the SEM was not explicitly mentioned, it was calculated from the data in the given publication. In the case of the total area of area 17 (Anderson et al., 1988), the authors only reported the mean and the range of values. The estimation of the error was done by calculating the mean distance between the maximum/minimum and the mean divided by the square root of the number of hemispheres. We estimated the error for the volume of the A lamina of the dLGN and of the volume of injection sites by reconstructing them by two individuals.

RESULTS

Light microscopy

Four cats were used, and 14 injections into the A laminae were recovered. All the ionophoretic injections of BDA into the dLGN were clearly visible in the light microscope after appropriate histology (Fig. 2). The reaction end-product at the injection site was too dark to be able accurately to count all neurons. The sections of the dLGN were counterstained with neutral red to make the lamina borders visible. All of the dLGN injections used for analysis were largely contained within the contralateral A lamina. Because the dLGN axons project retinotopically to area 17, each injection in the dLGN could be assigned to a specific region with labeled axons in area 17. The axons from each A lamina injection could be identified in area 17, where they formed a dense cluster of terminals and boutons in layer 4 (Fig. 3), and a few collaterals in layer 6. Rarely were retrogradely labeled corticothalamic cells found in layer 6, but, to prevent any possible contamination of labeled axon from retrogradely labeled corticothalamic cells, we made sure that none of the layer 4 sampling sites chosen for synapse counting was located above layer 6 neurons. Boutons and unmyelinated axons could be followed undiminished in the intensity of staining through the thickness of the section (Fig. 3D), indicating complete penetration of the reagents.

Densities of asymmetric synapses in layer 4 of area 17

We counted all asymmetric synapses, BDA labeled and unlabeled, and obtained an estimation of the density of asymmetric synapses in layer 4 that varied from 5×10^8 to 7.7×10^8 synapses/mm³. All the counts of asymmetric synapses were made using the physical disector method and are shown in Table 2. The shrinkage correction used in Table 2 is not obtained from each of the tissue samples but is the average

TABLE 1. Summary of Numerical Data on the Number of dLGN Relay Neurons and the Size of Their Arbor in Area 17¹

1	Number of relay neurons in the contralateral A lamina of the dLGN (\pm SEM)	186,900 \pm 1,430	Madarasz et al., 1978a,b
2	Ratio X:Y neurons	2:1	Friedlander et al., 1981; LeVay and Ferster, 1977
3	Number of X relay neurons in A lamina	124,600	2/3 \times row 1
4	Number of Y relay neurons in A lamina	62,301	1/3 \times row 1
5	Mean \pm SEM surface area of X arbors (only boutons, no gaps, in mm ²) (range)	0.8 \pm 0.04 (0.6–0.9)	Humphrey et al., 1985a
6	Mean \pm SEM surface area of Y arbors (only boutons, no gaps, in mm ²) (range)	1.1 \pm 0.08 (0.7–1.2)	Humphrey et al., 1985a
7	Total area of area 17 (\pm estimated SEM) (mm ²)	399 \pm 12.4	Anderson et al., 1988

¹The means and error were used for the calculation of the estimations presented in Table 4.

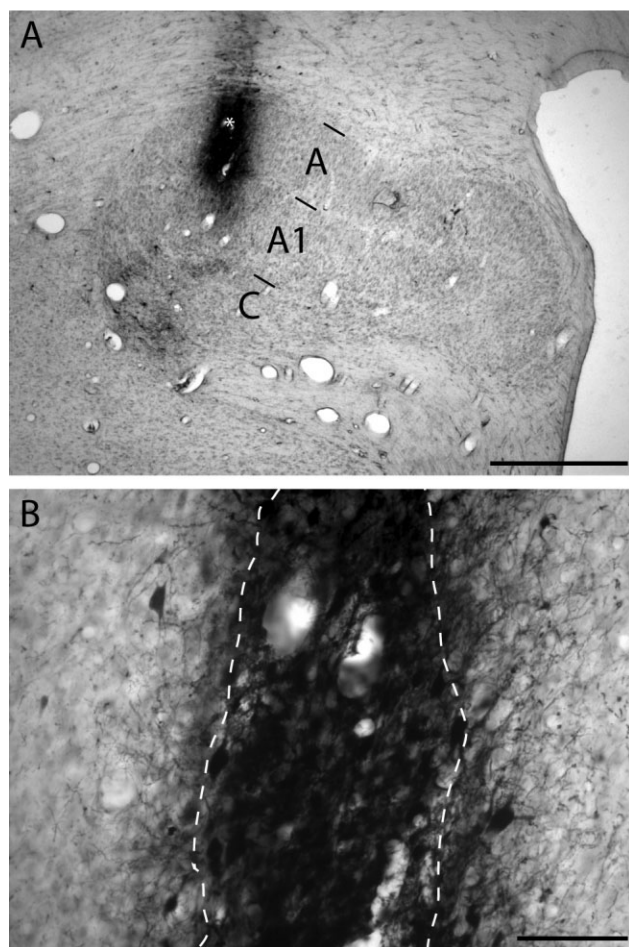


Figure 2. Light micrographs of BDA injection in the contralateral A lamina. **A:** Coronal section through the dLGN of the cat counterstained with neutral red. The asterisk indicates the BDA injection site located in lamina A. Laminae are indicated to the right. **B:** High-power micrograph of the injection site. The region inside the dotted line is defined as the core of the injection site. Scale bars = 1 mm in A; 100 μ m in B.

shrinkage measured repeatedly in our standard laboratory protocols.

The number of synapses per disector obtained with the URS and “strips” scheme followed a normal distribution (verified with the Lillie test), and the distribution of synapses counted using SRS was not significantly different from an array of random numbers chosen from a Poisson distribution with the same mean and size. The latter case was a result of the small size of the disector frame, which produced many disectors in which few or no synapses disappeared between the reference

and the lookup sections. In both animals, the medians of the samples collected with URS/strips were not different from those collected with SRS (cat 2003, $P = 0.59$; cat 1804, $P = 0.94$; Wilcoxon two-sampled test). Although the results obtained with the several sampling schemes produce similar results, the higher efficiency of the SRS allows us to sample more uniformly from each section and from a larger number of sections within a reasonable time.

The results in Table 2 indicate that the younger cat (cat 2003) had a higher density of asymmetric synapses than did the adults, but statistically this was not significantly different from the values for adult animals. The fact that cats at the age of 9 weeks have higher densities of synapses in layer 4 than adults has been shown in previous studies (Cragg, 1975; Winfield, 1981, 1983). We wanted to compare our total counts with the data in the adult cat from Beaulieu and Colonnier (1985), so we calculated the mean density of asymmetric synapses only from adult cats (cats 0904, 1604, and 1804). The mean density of asymmetric synapses in the adult was $5.9 \times 10^8 \pm 0.9 \times 10^8$ synapses/mm³ (mean \pm STD, $n = 4$ sampled regions, from three cats). When the sampled volume is corrected for shrinkage (resulting from fixation) of 11%, the density of asymmetric synapses was $4.1 \times 10^8 \pm 0.8 \times 10^8$ synapses/mm³ (mean \pm SD, $n = 4$ sampled regions, from three cats). The postfixation histological procedures may also induce shrinkage of the tissue; however, with our protocols this was negligible.

Estimation of the density of dLGN synapses in layer 4

In three of the cats, the four most strongly labeled sites in layer 4 were selected for the disectors (Fig. 3A). We assumed that all synapses formed by labeled boutons (Fig. 4) in the EM physical disectors were provided by the dLGN axons. The physical disectors were collected from the region in layer 4 where the densest dLGN label was found. This region was chosen qualitatively by two observers or, in case of doubt, by performing bouton counts with optical disectors.

The location of sampling sites was selected by using the RESORS scheme (da Costa et al., 2009) so that the only sampling sites photographed were those with labeled boutons (cat 0904 sample 1) or those where the labeled bouton formed a synapse (cat 0904 sample 2, cat 1804, cat 2003). The latter strategy produced an overestimation of the total number of asymmetric synapses in the neuropil, so we used instead the SRS sampling scheme to obtain this density.

Figure 5A shows a reference section of one of the disectors, with arrowheads indicating all the asymmetric synapses appearing in the section. Figure 5B is a magnified portion of Figure 5A and shows in more detail the synapses formed by a labeled bouton. Also indicated are the synapses that were not present in the lookup section (open arrowheads) and the

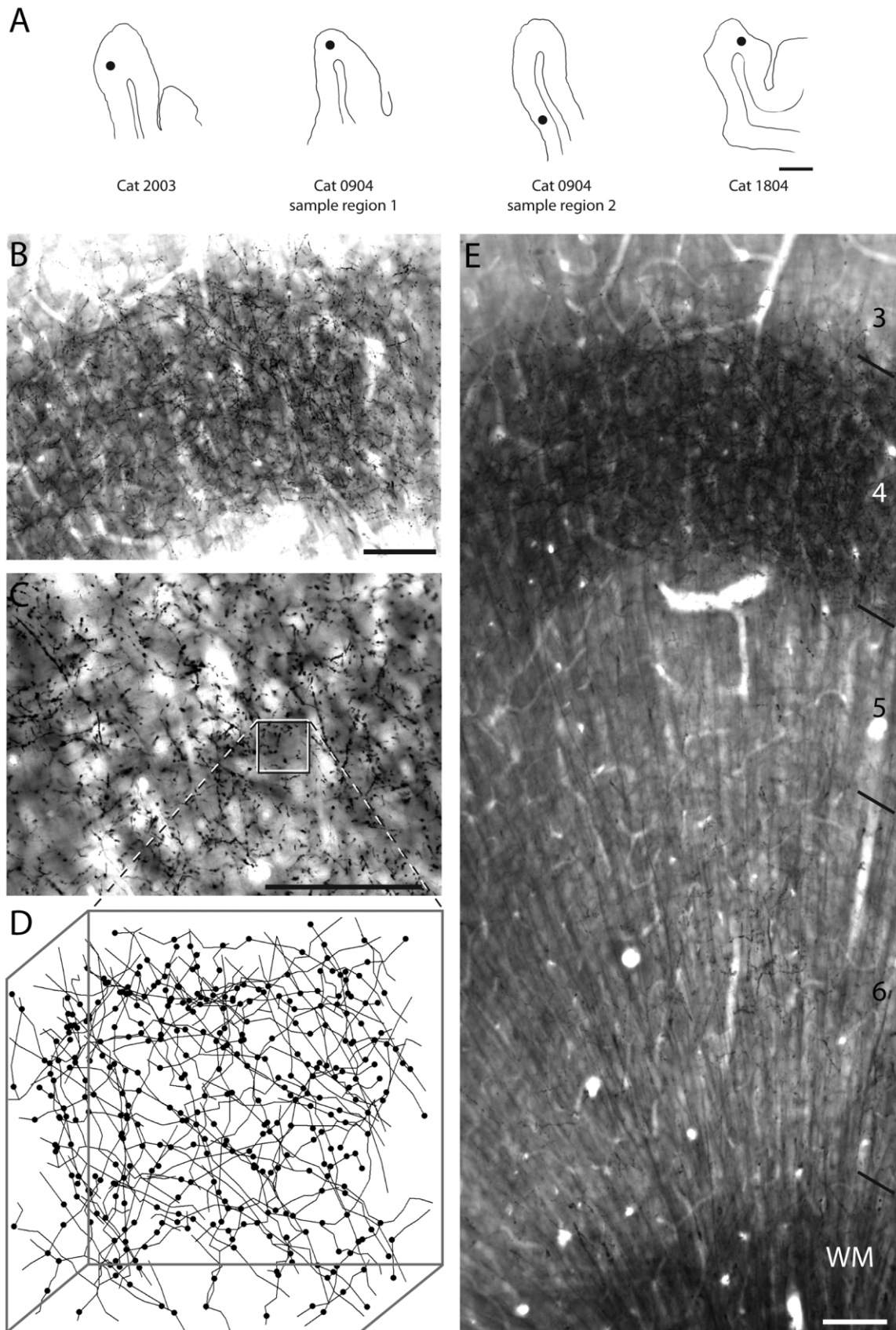


Figure 3. dLGN axons in area 17. **A:** Outline of coronal sections of cat area 17. For each cat, the black dot indicates the region of area 17 from which the dLGN input was quantified. **B,C,E:** Light micrographs of a coronal section of area 17 showing the clusters of dLGN axons at three different magnifications. **D:** LM reconstruction of all the dLGN axons in a volume of $30\ \mu\text{m} \times 30\ \mu\text{m} \times 80\ \mu\text{m}$. The dots indicate the location of axon varicosities. Scale bars = $100\ \mu\text{m}$.

TABLE 2. Densities of Asymmetric Synapses in Layer 4 of Area 17 [Shrinkage Correction (SC) of 11%]

Cat (sample region)	No. of disectors	Density mean ± SEM (×10 ⁸) (synapses/mm ³)	Density (SC) mean ± SEM (×10 ⁸) (synapses/mm ³)	Sampling method
2003	11	6.6 ± 0.4	4.7 ± 0.3	Strips
2003	72	7.7 ± 0.6	5.4 ± 0.4	SRS
0904 (1)	12	5.3 ± 0.4	3.7 ± 0.3	Strips/URS
0904 (2)	60	7.1 ± 0.7	5 ± 0.4	SRS
1604	4	5.0 ± 0.3	3.5 ± 0.2	URS
1804	4	5.8 ± 0.3	4.1 ± 0.2	URS
1804	80	6.3 ± 0.5	4.4 ± 0.4	SRS

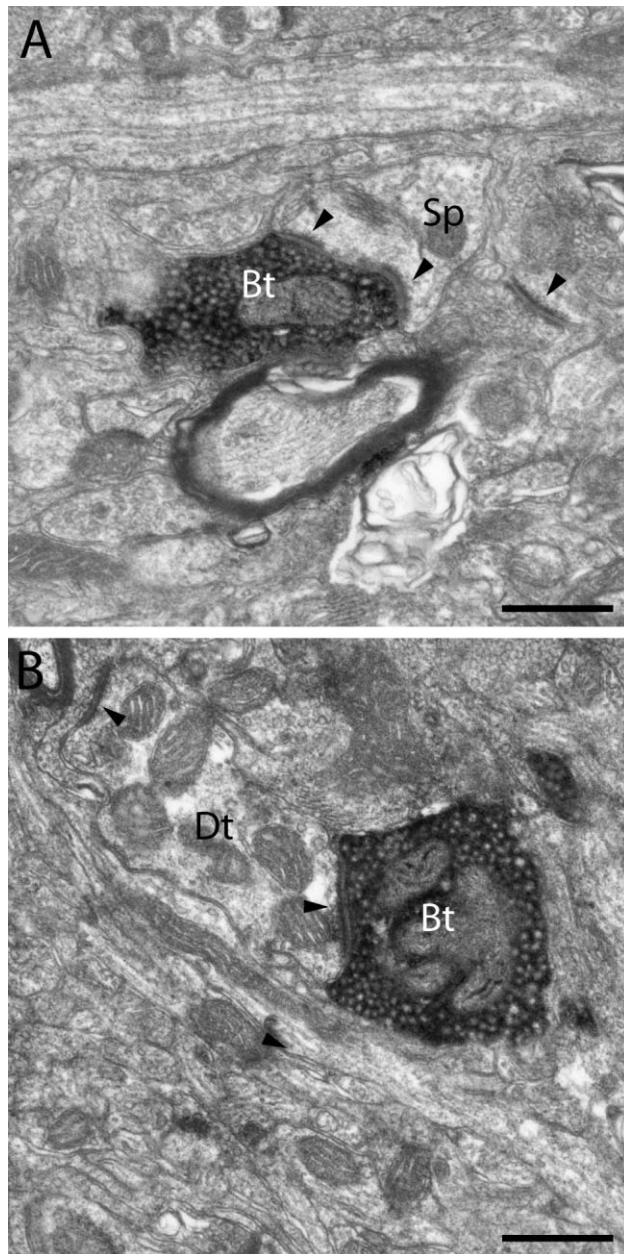


Figure 4. Electron micrographs of labeled dLGN boutons (Bt) and their targets in layer 4 of area 17. A: Bouton forming synapse with a dendritic spine (Sp). B: Bouton targeting the dendritic shaft of a putative inhibitory neuron. Postsynaptic densities are indicated by arrowheads. Scale bars = 0.5 μm.

synapses that were present in both sections (solid arrowheads), which were thus not counted. The density of dLGN synapses investigated in three cats varied between 0.09×10^8 and 0.21×10^8 synapses/mm³ (Table 3). This is 1.4% and 2.1% (cat 0904), 2.4% (cat 0904), and 2.8% (cat 2003) of all asymmetric synapses in layer 4.

Estimation of number of dLGN neurons in injection site

In the previous section, we calculated the percentage of asymmetric synapses formed by the dLGN axons in layer 4. We then needed to estimate whether the dLGN injections labeled all the relay neurons projecting to the sampled site in area 17. We started by estimating the number of labeled neurons in the injection site in the dLGN by reconstructing in 3-D the core of the injection site and also the contralateral A lamina (Fig. 6).

From the 3-D reconstructions, we calculated the volume of the injection site and of the A lamina (Table 4). We then calculated the proportion of the volume of the contralateral A lamina that was labeled by the injection. By using the number of relay cells in the A lamina determined by Madarasz et al. (1978a,b; Table 1), we could estimate what proportion of these cells was present in the volume of the core of the injection site.

The estimation of the number of dLGN relay neurons that are expected to form boutons in the region from which we sampled the disectors was calculated using the numerical data shown in Table 1. We estimated the mean expected number of X cells contributing boutons to our sample region to be 531 ± 31 (±SEM) and the mean expected number of Y cells to be 361 ± 31 (±SEM).

We then calculated a correction factor to our densities in the following way:

$$Correction\ Factor = \frac{\frac{531}{X} + \frac{361}{Y}}{2}$$

where X is the estimated number of labeled X relay neurons in the injection site, and Y is the estimated number of Y relay neurons. The correction factor was 1.12 for cat 2003, 4.59 for sample region 1 of cat 0904 and 4.93 for sample region 2, and 2.09 for cat 1804 (Table 4). After correction, the mean percentage of synapses in layer 4 of area 17 formed by the dLGN was $6\% \pm 2.7\%$ (±SD). Note that, for every value used in the estimation, we also estimated the accompanying error. The errors were then combined in quadrature. The mean error of the estimation (mean of the SEMs in line 8 of Table 4) was 2%.

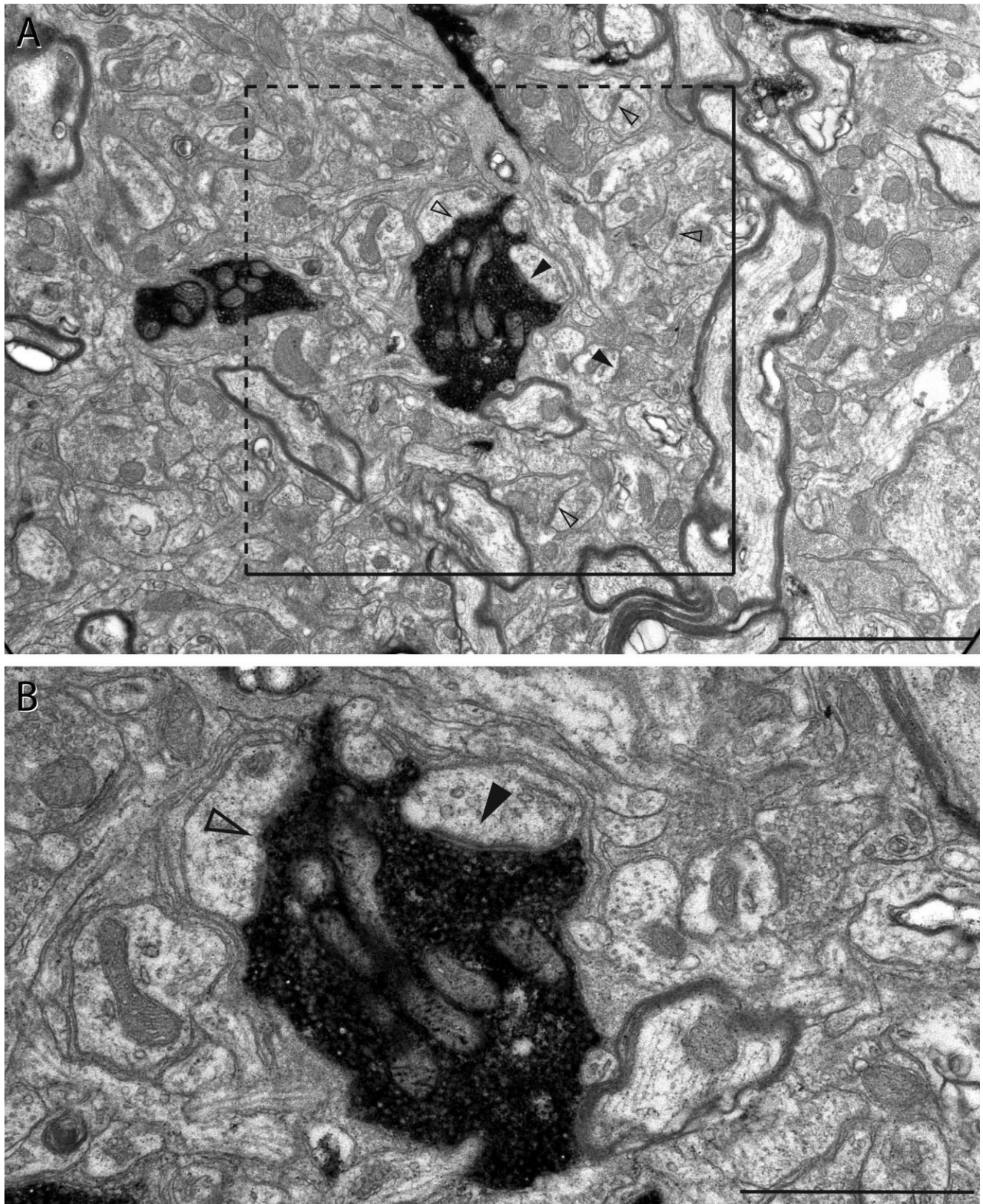


Figure 5.

A: Electron micrograph of the reference section of a physical disector. The disector frame is shown in black; the solid lines represent the forbidden edges and the dashed lines the acceptance edges. Synapses disappearing from the reference to the lookup section are indicated by solid arrowheads. Synapses present in both sections are indicated by open arrowheads. **B:** Magnification of a portion of the reference section in A showing synapses formed by a dLGN. Scale bars = 1 μm.

TABLE 3. Density of Labeled dLGN Synapses in the Neuropil of Layer 4 of Area 17

Cat (sample region)	No. of disectors	Mean No. of dLGN synapses per disector	Density of dLGN synapses mean \pm SEM ($\times 10^8$) (synapses/mm ³)
2003	279	0.0645	0.21 \pm 0.05
0904(1)	351	0.0285	0.09 \pm 0.03
0904(2)	328	0.0305	0.10 \pm 0.03
1804	367	0.0463	0.15 \pm 0.04

DISCUSSION

The major goal of this study was to determine the proportion of asymmetric synapses formed by the dLGN boutons in layer 4 of area 17 of the cat and to avoid the methodological shortcomings of all previous estimates by using an unbiased stereological method and correcting for the size of the injection. Our new estimate of 6% falls within the values of previous studies that indicate that the thalamic input contributes a small proportion of the asymmetric synapses in layer 4 (Garey and Powell, 1971; Hornung and Garey, 1981; LeVay, 1986). Although our procedure addresses previous problems of accuracy, it is dependent on the coverage factors of X and Y axons (Humphrey et al., 1985) and on the densities of cells in the dLGN (Madarasz et al., 1978a,b). Thus, together with our estimate of the thalamic input, we made an estimate of the uncertainty of our measure, which combines the standard errors of our sampling and of the values used from the literature. It is also quite remarkable that studies that are based not on neuronal tracers but on numerical analysis of quantitative neuroanatomy (Peters and Payne, 1993), or morphological identification of different presynaptic terminals (Ahmed et al., 1994), produce results very similar to ours.

In previous experiments addressing this same question, LeVay (1986), like ourselves, used local injections of an anterograde neuronal tracer, in this case wheat germ agglutinin (WGA), rather than degeneration methods. However, if the injection in the dLGN is not large enough to label all the relay neurons, it will lead to an underestimate of dLGN synapses in the cortex. Thus, we have measured the size of the tracer uptake zone in the dLGN and scaled our estimates proportionally. The histological procedure used by LeVay (1986) to reveal the WGA-HRP induces voids in the boutons, which is the indication that the tracer is present. Because these voids are smaller than the boutons, and because LeVay used single sections to count synapses, we would expect some underestimation. The degeneration method used by Garey and Powell (1971) and Hornung and Garey (1981) avoids the use of a tracer but has the disadvantage that the survival time after lesion has to be timed correctly so that some degenerating terminals do not undergo phagocytosis while others are still degenerating (for review see Ralston, 1990), which will lead to an underestimation. In all of the above-described work, counts were performed in single sections, and this can lead to a bias toward larger synapses. EM autoradiography combined with the uptake of radioactive labeled amino acids has the advantage of being very sensitive (for review see White, 1979). However, the L-[2,3-³H]proline used in the work of LeVay and Gilbert (1976) is also transported retrogradely (LeVay and Sherk, 1983) and thus may possibly label terminals from layer 6 pyramidal neurons, which also arborize in layer 4. This would lead to an overestimation of the dLGN synapses. Moreover, L-[2,3-³H]proline has been used to investigate the projection

from the eye to the primary visual cortex (Grafstein and Lauro, 1973; Wiesel et al., 1974), because it is transported transneuronally (Grafstein, 1971). Thus, after injections into the dLGN, one cannot rule out that the L-[2,3-³H]proline passed across the thalamocortical synapse in layer 4 of area 17 and labeled cortical neurons and their axons, thus inducing an overestimation of the percentage of dLGN synapses. Another source of overestimation with this technique is that there is some scatter of the radioactivity, giving rise to a background of silver grains that might lead to false positives. These three defects most likely led to an overestimation of the number of dLGN boutons in layer 4 of area 17 by LeVay and Gilbert (1976). In fact, in a later publication, LeVay (1986) acknowledges that the 28% reported in his study with Gilbert might be an overestimation, because no procedure was used to subtract background label.

The major drawback with all tracer techniques is that they do not guarantee that all the dLGN neurons that contribute boutons to a sampling site in area 17 are completely labeled. In the monkey, the dLGN relay cells contain parvalbumin, and this can be used as an intrinsic marker of thalamic boutons in primary visual cortex (Latawiec et al., 2000), where they form 6–10% of the layer 4 asymmetric synapses. However, no intrinsic marker has been found for cat thalamic relay neurons, so tracers remain the only effective means of labeling the dLGN afferents in the cat. It is clear from reconstructions of single dLGN axons in area 17 (Freund et al., 1985b; Humphrey et al., 1985) that, although X axons form single clusters, Y axons can form more than one bouton cluster, so the terminal arborization spreads over millimeters. From our own injections, we can see one main cluster of boutons in layer 4 and, around it, less dense clusters. These less dense clusters could be the lateral projections of Y-axons or, if our injection was large enough, of X-axons innervating the “next” ocular dominance column. Both seem likely, because layer 4B, which receives input only from X-axons (Freund et al., 1985b; Humphrey et al., 1985), was also labeled in multiple clusters. The problem was to estimate the proportion of unlabeled neurons. We estimated this fraction by obtaining a ratio between the number of dLGN relay neurons that would contribute boutons to our sampling area based on their coverage area and the number of neurons that were expected to be labeled in the volume of our injection site in the dLGN. We then scaled our estimation of dLGN synapses in area 17 by this ratio.

Density of synapses in layer 4 of area 17 of the cat

To discover the proportion of dLGN synapses in the neuropil of layer 4 of area 17 also requires that we know the number or proportion of the non-dLGN asymmetric synapses. We found that the density of the asymmetric synapses in layer 4 of area 17 is 5.9×10^8 synapses/mm³ when no correction for

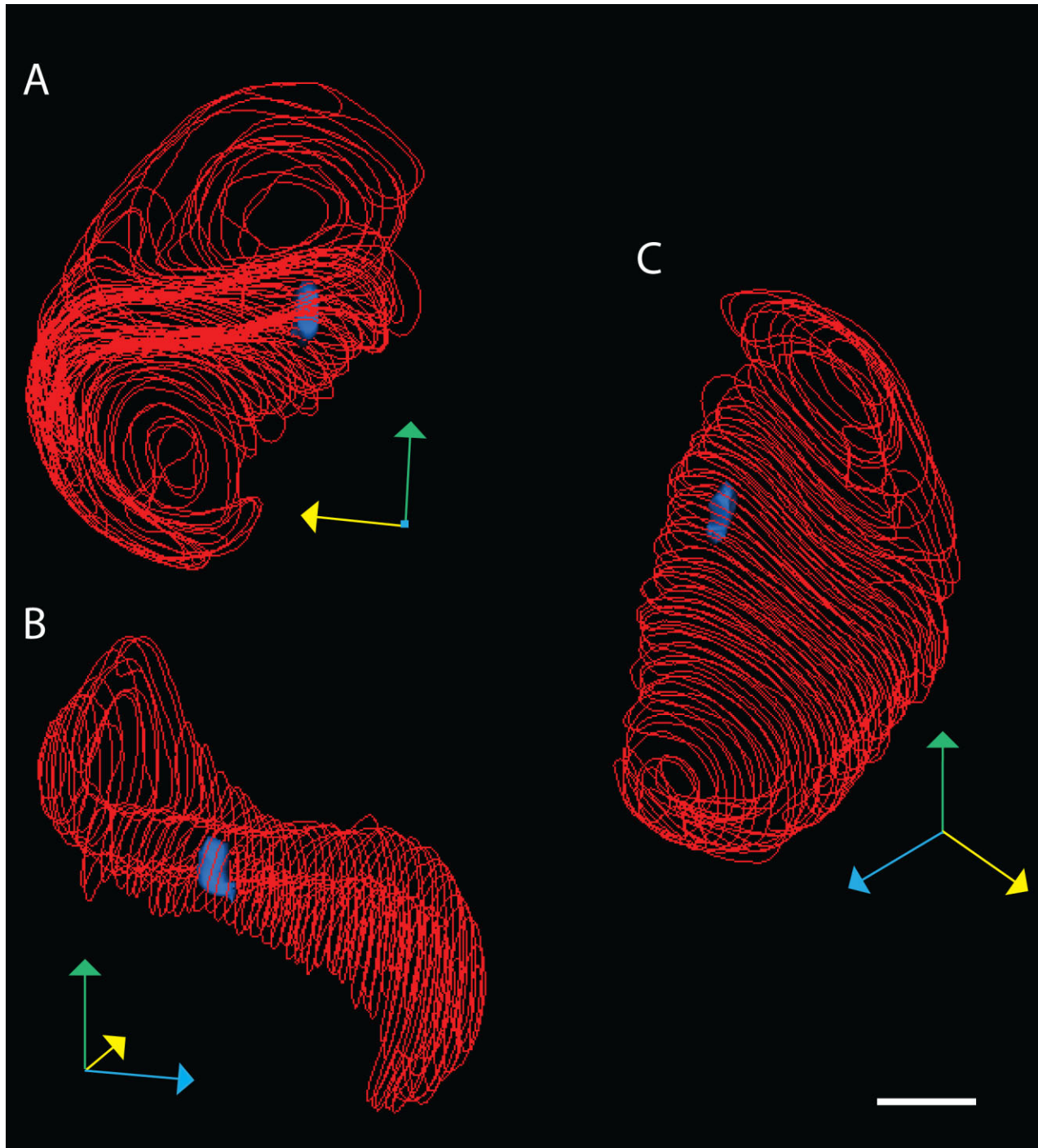


Figure 6. Reconstruction of the contralateral A lamina of the dLGN from light micrographs taken from serial 80- μm sections. The contours of the A lamina are indicated in red. We show the reconstruction of one injection site (in blue) inside the A lamina. **A:** Front view. **B:** Side view. **C:** Top view. The arrows indicate the orientation of the reconstruction: green indicates dorsal; blue indicates posterior; yellow indicates lateral. Scale bar = 1 mm.

shrinkage is applied, but this falls to 4.1×10^8 synapses/ mm^3 when a correction for fixation shrinkage is applied. We give both values, because, although the second is the more correct description of the *in vivo* situation, this type of shrinkage correction is rarely used in morphological and topographic

descriptions of reconstructed neurons. Because of this the value of 5.9×10^8 synapses/ mm^3 is the more useful for comparison with published data.

Previous estimates of the number of asymmetric synapses in area 17 of the cat (Beaulieu and Colonnier, 1985; Cragg,

TABLE 4. Volume and Number of Neurons in the Injection Sites¹

		Cat 2003	Cat 0904 (sample 1)	Cat 0904 (sample 2)	Cat 1804
1	Volume of injection site (\pm SEM) (mm ³).	0.034 \pm 0.0001	0.007 \pm 0.002	0.007 \pm 0.0004	0.019 \pm 0.004
2	Volume of contralateral A lamina of the dLGN (\pm SEM) (mm ³).	7.614 \pm 0.016	6.670 \pm 0.014(a)	6.670 \pm 0.014(a)	7.987 \pm 0.017(a)
3	Proportion of A lamina occupied by injection site (\pm SEM), line 1/line 2	0.0045 \pm 0.00002	0.0011 \pm 0.0004	0.0010 \pm 0.0001	0.0024 \pm 0.0004
4	Estimation of relay cell number in injection site (\pm SEM), line 3 \times Table 1, line 1	844 \pm 8	205 \pm 68	191 \pm 12	450 \pm 83
5	Estimation of X cell number in injection site (\pm SEM), line 4 \times 2/3	563 \pm 5	137 \pm 45	127 \pm 8	300 \pm 56
6	Estimation of Y cell number in injection site (\pm SEM), line 4 \times 1/3	281 \pm 3	68 \pm 23	64 \pm 4	150 \pm 28
7	Correction factor (\pm SEM)	1.12 \pm 0.06	4.59 \pm 1.11	4.93 \pm 0.35	2.09 \pm 0.30
8	Percentage of asymmetric synapses formed by dLGN boutons \times line 7 (\pm SEM).	2.8 \pm 0.7	9.2 \pm 3.7	7.1 \pm 2.6	5.1 \pm 1.6

¹Estimation of the number of neurons in the injection sites that generated the cortical clusters analyzed with the disector method. In cats 0904 and 1804, the injection site was formed by two injections in close apposition. The volume was not corrected for any shrinkage.

²In cats 0904 and 1804, the very posterior tip of the dLGN was not reconstructed.

1975; Winfield, 1981) have been challenged as being biased (Mayhew, 1996). In the present study, we used the unbiased physical disector method (Sterio, 1984), now considered to be the “gold standard” technique for counts, because it is independent of the size, shape, and distribution of the synapses counted (for review see Mayhew, 1996). The estimated density of asymmetric synapses presented in this work is higher than that of Beaulieu and Colonnier (1985) for the same region of area 17 of the cat. Even though there are obvious advantages of the disector technique compared with the model-based counting methods used by Beaulieu and Colonnier (1985), the closeness of the two estimates and the variance in sampling and between animals suggest that the biases inherent in the counts of Beaulieu and Colonnier (1985) are not significant. DeFelipe et al. (1999) actually performed an experimental comparison between the two techniques in human cerebral cortex and found no significant differences between the two. We have also applied the methods of Beaulieu and Colonnier (1985) to some of the single section counts performed in the reference and lookup sections in two animals, and, even though the densities were both lower, they were not significantly different from the disector results.

A potentially important difference in the detail of the methods used by Beaulieu and Colonnier (1985) is that of the shrinkage correction. Beaulieu and Colonnier (1985) observed and corrected for shrinkage resulting from histological procedures that varied between 12% and 19%, but their tissue did not undergo any shrinkage from perfusion with fixative. The brains of the cats used in the present study did shrink slightly during perfusion, but the shrinkage resulting from histological procedures was found to be negligible. Even though the protocols used by Beaulieu and Colonnier (1985) and ours induce shrinkage of the tissue in different steps of the procedure, the net shrinkage is very similar in the two studies.

The shrinkage is potentially a major confounding variable in estimating the density of synapses, which is a crucial number underlying experimental and theoretical work dedicated to solving the circuit diagram of the cortex (see, e.g., Binzegger et al., 2004, regarding area 17 of the cat). Even though densities are commonly reported in the literature, this measure is not optimal for two reasons. First, density is sensitive to volume artifacts (such as shrinkage). A better practice would be to indicate the total number of synapses in layer 4 of area 17. Second, theoretical models tend to use the total numbers

instead of densities, and usually one needs to compile data from different laboratories with different histological procedures (and hence potentially different tissue shrinkages) to obtain such numbers. Although the well-publicized advances in the automation of EM promise that problems such as counting synapses will be revisited with less effort, these methods will be confined to very small volumes of tissue and the difficulties of obtaining quantitative data on long-distance connections, such as the thalamocortical or corticocortical, remain.

Functional implications

In their original model of layer 4 simple cells in the cat, Hubel and Wiesel (1962) assumed that all the excitation arises from the dLGN afferents. Support for their interpretation has come from cross-correlation studies by Reid and colleagues (Alonso et al., 2001; Reid and Alonso, 1995), in which, by implication, all the postsynaptic spikes could be accounted for by a spike in a presynaptic dLGN relay cell. Another, basically concordant study estimated that the dLGN provides of 35–46% of the functional visual input to layer 4 simple cells (Chung and Ferster, 1998; Ferster et al., 1996). Their indirect estimate was made on the basis of changes in the amplitude of intracellular potentials during periods when cortical activity was suppressed either by cortical cooling or by electrical stimulation. Although functionally dominant during visual stimulation, the thalamic input is nevertheless represented by a small fraction of layer 4 synapses, as the present study confirms. The anatomical maps of the synapses on the dendrites of the spiny stellate cells in layer 4 made by Ahmed et al. (1994) indicated that the dominant excitatory input in layer 4 arises from local pyramidal neurons in layer 6 (~45%) and other layer 4 spiny stellates (~28%). This experimental result agrees with estimates of cortical connectivity based on the known anatomical data (Binzegger et al., 2004; Peters and Payne, 1993), which also point to the fact that most of the input to any cortical neuron comes from its neighbors. Slice recordings from neurons in layer 4 of cat area 17 (Stratford et al., 1996; Tarczy-Hornoch et al., 1999) provided a comparison of the amplitudes, efficacy, and dynamics of thalamocortical and corticocortical synapses. The conclusion from these *in vitro* studies was that the predominant excitatory input to simple cells in layer 4 came from other cortical neurons, not from the dLGN (Douglas et al., 1996).

Douglas and Martin (1991) and Douglas et al. (1989) proposed a reconciliation of the model of Hubel and Wiesel (1962) with the experimental data of a small thalamic input to layer 4. They emphasized the importance of the recurrent circuits formed by the local cortical neurons in amplifying the dLGN input. In their view, the number of dLGN synapses is necessarily small, because otherwise a stimulus of nonoptimal orientation will also drive the simple cells, since the dLGN inputs are not orientation sensitive. Douglas and Martin (2007) proposed that the dLGN input is “just enough” to drive their targets in layer 4 only when the correctly oriented stimulus is presented, as required by the Hubel and Wiesel model, and that this input is then amplified by the recurrent circuits of the cortex. Recently, Banitt et al. (2007), developed a detailed and biophysically realistic model of a spiny stellate cell and showed that the small numbers of dLGN synapses formed on each layer 4 spiny stellate cell are, on their own, insufficient to drive them adequately. However, the model showed that, if the simple cells were depolarized by spontaneous excitatory input from cortical neurons and the dLGN synapses were activated synchronously, then they were indeed “just enough” to drive the cortical neurons.

These studies indicate that, if the concept of “just enough” (Douglas and Martin, 2007) is to be properly modeled and then tested experimentally, accurate numbers are essential. Our count is another step toward an accurate determination of the input to layer 4 neurons in cat visual cortex. However, knowing the number of dLGN synapses a neuron receives is not enough: we still have to determine whether these synapses are equally distributed across all the dendrites in a “Peters-rule” manner (Binzegger et al., 2004; Braitenberg and Schüz, 1991; Peters and Feldman, 1976) or whether different cell types receive more or less of the thalamic input, as in “White’s exceptions” (Benshalom and White, 1986; Braitenberg and Schüz, 1991; White and Hersch, 1981; White and Rock, 1981). Peters Rule predicts that each spiny stellate cell receives about 100 dLGN synapses (Binzegger et al., 2004; Peters and Payne, 1993). On the basis of a combination of cross-correlation data and the coverage factor of the dLGN receptive, Alonso et al. (2001) estimated that ~30 dLGN neurons project to a spiny stellate cell. To achieve the 100 synapses estimated from the Peters rule means that the 30 single afferents would have to make multiple synapses with each spiny stellate cell. Structural evidence for multiple synapses comes from Freund et al. (1985a), who found as many as eight synapses from a single afferent to single cortical neurons. However, their method confined them to the analysis of single 80- μ m-thick sections and so most likely underestimated the number of multiple synapses each afferent forms.

Our knowledge of the location of the dLGN synapses on the dendritic tree, their size, and their receptor composition remains surprisingly fragmentary. However, the data presented here strongly support a general principle of cortical connectivity, where wiring is optimized by making dense local connections and sparse long-distance connections. Inevitably, this places the weight of cortical computation on the local circuits (Douglas and Martin, 2007).

ACKNOWLEDGMENTS

We thank Rita Bopp and German Koestinger for their expert technical assistance and John Anderson for his helpful com-

ments on the manuscript. We also thank Dr. Clermont Beaulieu for helpful discussions on synapse sampling.

LITERATURE CITED

- Ahmed B, Anderson JC, Douglas RJ, Martin KA, Nelson JC. 1994. Polyneuronal innervation of spiny stellate neurons in cat visual cortex. *J Comp Neurol* 341:39–49.
- Ahmed B, Anderson JC, Martin KA, Nelson JC. 1997. Map of the synapses onto layer 4 basket cells of the primary visual cortex of the cat. *J Comp Neurol* 380:230–242.
- Alonso JM, Usrey WM, Reid RC. 2001. Rules of connectivity between geniculate cells and simple cells in cat primary visual cortex. *J Neurosci* 21:4002–4015.
- Anderson PA, Olavarria J, Van Sluyters RC. 1988. The overall pattern of ocular dominance bands in cat visual cortex. *J Neurosci* 8:2183–2200.
- Banitt Y, Martin KA, Segev I. 2007. A biologically realistic model of contrast invariant orientation tuning by thalamocortical synaptic depression. *J Neurosci* 27:10230–10239.
- Beaulieu C, Colonnier M. 1985. A laminar analysis of the number of round-asymmetrical and flat-symmetrical synapses on spines, dendritic trunks, and cell bodies in area 17 of the cat. *J Comp Neurol* 231:180–189.
- Benshalom G, White EL. 1986. Quantification of thalamocortical synapses with spiny stellate neurons in layer IV of mouse somatosensory cortex. *J Comp Neurol* 253:303–314.
- Binzegger T, Douglas RJ, Martin KA. 2004. A quantitative map of the circuit of cat primary visual cortex. *J Neurosci* 24:8441–8453.
- Braitenberg V, Schüz A. 1991. Peters’ rule and White’s exceptions. *Anatomy of the cortex*. Berlin: Springer.
- Chung S, Ferster D. 1998. Strength and orientation tuning of the thalamic input to simple cells revealed by electrically evoked cortical suppression. *Neuron* 20:1177–1189.
- Colonnier M. 1968. Synaptic patterns on different cell types in the different laminae of the cat visual cortex. An electron microscope study. *Brain Res* 9:268–287.
- Cragg BG. 1975. The development of synapses in the visual system of the cat. *J Comp Neurol* 160:147–166.
- Crick F, Koch C. 1998. Constraints on cortical and thalamic projections: the no-strong-loops hypothesis. *Nature* 391:245–250.
- da Costa NM, Hepp K, Martin KA. 2009. A systematic random sampling scheme optimized to detect the proportion of rare synapses in the neuropil. *J Neurosci Methods* (in press).
- DeFelipe J, Jones EG. 1991. Parvalbumin immunoreactivity reveals layer IV of monkey cerebral cortex as a mosaic of microzones of thalamic afferent terminations. *Brain Res* 562:39–47.
- DeFelipe J, Marco P, Busturia I, Merchán-Pérez A. 1999. Estimation of the number of synapses in the cerebral cortex: methodological considerations. *Cereb Cortex* 9:722–732.
- Douglas RJ, Martin KA. 1991. A functional microcircuit for cat visual cortex. *J Physiol* 440:735–769.
- Douglas RJ, Martin KA. 2007. Mapping the matrix: the ways of neocortex. *Neuron* 56:226–238.
- Douglas RJ, Martin KA, Whitteridge D. 1989. A canonical microcircuit for neocortex. *Neural Comput* 1:480–488.
- Douglas RJ, Mahowald M, Martin KA, Stratford KJ. 1996. The role of synapses in cortical computation. *J Neurocytol* 25: 893–911.
- Ferster D, Chung S, Wheat H. 1996. Orientation selectivity of thalamic input to simple cells of cat visual cortex. *Nature* 380:249–252.
- Fiala JC. 2005. Reconstruct: a free editor for serial section microscopy. *J Microsc* 218:52–61.
- Freund TF, Martin KA, Somogyi P, Whitteridge D. 1985a. Innervation of cat visual areas 17 and 18 by physiologically identified X- and Y-type thalamic afferents. II. Identification of postsynaptic targets by GABA immunocytochemistry and Golgi impregnation. *J Comp Neurol* 242: 275–291.
- Freund TF, Martin KA, Whitteridge D. 1985b. Innervation of cat visual areas 17 and 18 by physiologically identified X- and Y-type thalamic afferents. I. Arborization patterns and quantitative distribution of postsynaptic elements. *J Comp Neurol* 242:263–274.
- Friedlander MJ, Martin KA. 1989. Development of Y-axon innervation of cortical area 18 in the cat. *J Physiol* 416:183–213.
- Garey LJ, Powell TP. 1971. An experimental study of the termination of the

- lateral geniculo-cortical pathway in the cat and monkey. *Proc R Soc Lond B Biol Sci* 179:41–63.
- Grafstein B. 1971. Transneuronal transfer of radioactivity in the central nervous system. *Science* 172:177–179.
- Grafstein B, Laureno R. 1973. Transport of radioactivity from eye to visual cortex in the mouse. *Exp Neurol* 39:44–57.
- Gray EG. 1959. Axo-somatic and axo-dendritic synapses of the cerebral cortex: an electron microscope study. *J Anat* 93:420–433.
- Gundersen HJ, Jensen EB. 1987. The efficiency of systematic sampling in stereology and its prediction. *J Microsc* 147:229–263.
- Hollander H, Vanegas H. 1977. The projection from the lateral geniculate nucleus onto the visual cortex in the cat. A quantitative study with horseradish-peroxidase. *J Comp Neurol* 173:519–536.
- Hornung JP, Garey LJ. 1981. The thalamic projection to cat visual cortex: ultrastructure of neurons identified by Golgi impregnation or retrograde horseradish peroxidase transport. *Neuroscience* 6:1053–1068.
- Hubel DH, Wiesel TN. 1962. Receptive fields, binocular interaction and functional architecture in the cat's visual cortex. *J Physiol* 160:106–154.
- Humphrey AL, Sur M, Uhlrich DJ, Sherman SM. 1985. Projection patterns of individual X- and Y-cell axons from the lateral geniculate nucleus to cortical area 17 in the cat. *J Comp Neurol* 233:159–189.
- Kawano J. 1998. Cortical projections of the parvocellular laminae C of the dorsal lateral geniculate nucleus in the cat: an anterograde wheat germ agglutinin conjugated to horseradish peroxidase study. *J Comp Neurol* 392:439–457.
- Laemle LK. 1975. Cell populations of the lateral geniculate nucleus of the cat as determined with horseradish peroxidase. *Brain Res* 100:650–656.
- Latawiec D, Martin KA, Meskenaite V. 2000. Termination of the geniculocortical projection in the striate cortex of macaque monkey: a quantitative immunoelectron microscopic study. *J Comp Neurol* 419:306–319.
- LeVay S. 1986. Synaptic organization of claustral and geniculate afferents to the visual cortex of the cat. *J Neurosci* 6:3564–3575.
- LeVay S, Gilbert CD. 1976. Laminar patterns of geniculocortical projection in the cat. *Brain Res* 113:1–19.
- LeVay S, Sherk H. 1983. Retrograde transport of [³H]proline: a widespread phenomenon in the central nervous system. *Brain Res* 271:131–134.
- Leventhal AG. 1979. Evidence that the different classes of relay cells of the cat's lateral geniculate nucleus terminate in different layers of the striate cortex. *Exp Brain Res* 37:349–372.
- Maciewicz RJ. 1975. Thalamic afferents to areas 17, 18 and 19 of cat cortex traced with horseradish peroxidase. *Brain Res* 84:308–312.
- Madarasz M, Gerle J, Hajdu F, Somogyi G, Tombol T. 1978a. Quantitative histological studies on the lateral geniculate nucleus in the cat. II. Cell numbers and densities in the several layers. *J Hirnforsch* 19:159–164.
- Madarasz M, Gerle J, Hajdu F, Somogyi G, Tombol T. 1978b. Quantitative histological studies on the lateral geniculate nucleus in the cat. III. Distribution of different types of neurons in the several layers of LGN. *J Hirnforsch* 19:193–201.
- Mayhew TM. 1996. How to count synapses unbiasedly and efficiently at the ultrastructural level: proposal for a standard sampling and counting protocol. *J Neurocytol* 25:793–804.
- Peters A, Feldman ML. 1976. The projection of the lateral geniculate nucleus to area 17 of the rat cerebral cortex. I. General description. *J Neurocytol* 5:63–84.
- Peters A, Payne BR. 1993. Numerical relationships between geniculocortical afferents and pyramidal cell modules in cat primary visual cortex. *Cereb Cortex* 3:69–78.
- Ralston HJ 3rd. 1990. Analysis of neuronal networks: a review of techniques for labeling axonal projections. *J Elec Microsc Techniq* 15:322–331.
- Reid RC, Alonso JM. 1995. Specificity of monosynaptic connections from thalamus to visual cortex. *Nature* 378:281–284.
- Royet JP. 1991. Stereology: a method for analyzing images. *Prog Neurobiol* 37:433–474.
- Sanderson KJ. 1971. The projection of the visual field to the lateral geniculate and medial interlaminar nuclei in the cat. *J Comp Neurol* 143:101–108.
- Sherman SM, Guillery RW. 1998. On the actions that one nerve cell can have on another: distinguishing “drivers” from “modulators.” *Proc Natl Acad Sci U S A* 95:7121–7126.
- Slomianka L, West MJ. 2005. Estimators of the precision of stereological estimates: an example based on the CA1 pyramidal cell layer of rats. *Neuroscience* 136:757–767.
- Small JV. 1968. Measurement of section thickness. In: Bocciarelli EDS, editor. *Rome: Tipografia Poliglotta Vaticana*.
- Sterio DC. 1984. The unbiased estimation of number and sizes of arbitrary particles using the disector. *J Microsc* 134:127–136.
- Stratford KJ, Tarczy-Hornoch K, Martin KA, Bannister NJ, Jack JJ. 1996. Excitatory synaptic inputs to spiny stellate cells in cat visual cortex. *Nature* 382:258–261.
- Tarczy-Hornoch K, Martin KA, Stratford KJ, Jack JJ. 1999. Intracortical excitation of spiny neurons in layer 4 of cat striate cortex in vitro. *Cereb Cortex* 9:833–843.
- White EL. 1979. Thalamocortical synaptic relations: a review with emphasis on the projections of specific thalamic nuclei to the primary sensory areas of the neocortex. *Brain Res* 180:275–311.
- White EL, Hersch SM. 1981. Thalamocortical synapses of pyramidal cells which project from Sml to Msl cortex in the mouse. *J Comp Neurol* 198:167–181.
- White EL, Rock MP. 1981. A comparison of thalamocortical and other synaptic inputs to dendrites of two nonspiny neurons in a single barrel of mouse Sml cortex. *J Comp Neurol* 195:265–277.
- Wiesel TN, Hubel DH, Lam DM. 1974. Autoradiographic demonstration of ocular-dominance columns in the monkey striate cortex by means of transneuronal transport. *Brain Res* 79:273–279.
- Winfield DA. 1981. The postnatal development of synapses in the visual cortex of the cat and the effects of eyelid closure. *Brain Res* 206:166–171.
- Winfield DA. 1983. The postnatal development of synapses in the different laminae of the visual cortex in the normal kitten and in kittens with eyelid suture. *Brain Res Dev Brain Res* 9:155–169.